

INVARIANTS OF SELF-INTERSECTED AND INVERSIVE N-PERIODICS IN THE ELLIPTIC BILLIARD

RONALDO GARCIA AND DAN REZNIK

ABSTRACT. We study more invariants in the elliptic billiard, including those manifested by self-intersected orbits and inversive polygons. We also derive expressions for some entries in “Eighty New Invariants of N-Periodics in the Elliptic Billiard” (2020), *arXiv:2004.12497*.

Keywords invariant, elliptic, billiard.

MSC 51M04 and 37D50 and 51N20 and 51N35 and 68T20

1. INTRODUCTION

The two classic invariants of N-periodics in the elliptic billiard are perimeter L and Joachimsthal’s constant J . The former is a direct consequence of integrability whereas the latter is equivalent to stating that all trajectory segments are tangent to a confocal caustic [20]; see Figure 1.

It turns out constant L and J have often surprising cartesian manifestations. In [18] the following experimentally-found invariants were introduced: (i) the sum of N-periodic angle cosines was shown to be invariant; (ii) the ratio of outer (aka. tangential) polygon (see Figure 2) to the N-periodic’s is invariant if N is odd. These were soon elegantly proved using tools of algebraic and differential geometry [2, 4, 6]. For the $N = 3$ case some invariants have been explicitly derived [11].

Date: October 2020.

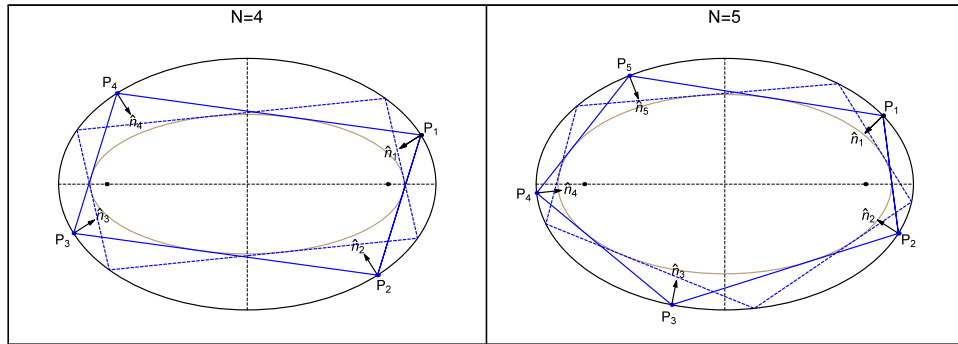


FIGURE 1. Elliptic Billiard (black) 4- and 5-periodics (blue). Every trajectory vertex P_i (resp. segment P_iP_{i+1}) is bisected by the local normal \hat{n}_i (resp. tangent to the confocal caustic, brown). A second, equi-perimeter member of each family is also shown (dashed blue). [Video](#).

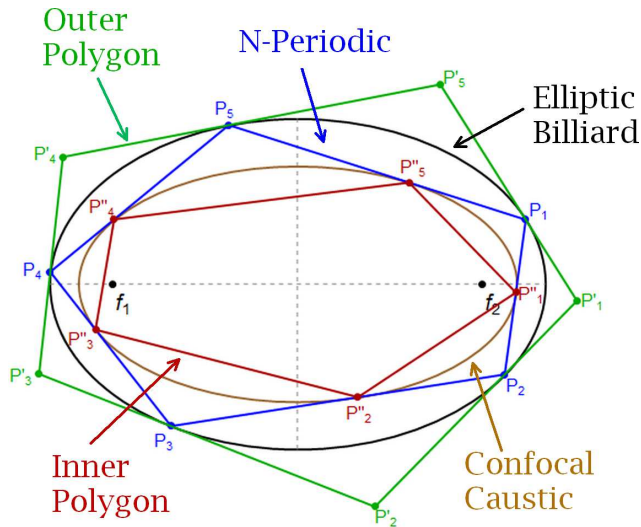


FIGURE 2. The N-periodic (blue), is associated with an outer (green) and an inner (red) polygons. The former's sides are tangent to the billiard (black) at each N-periodic vertex; the latter's vertices are the tangency points of N-periodics sides to the confocal caustic (brown). [Video](#)

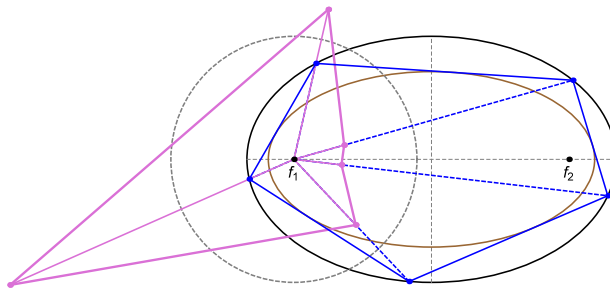


FIGURE 3. The inversive polygon (pink) has vertices at inversions of the P_i (blue polygon) with respect to a unit circle (dashed black) centered on f_1 . It turns out its perimeter is also invariant over the family as is the sum of its spoke lengths (pink lines) [Video](#).

Experimentation with additional polygons such as pedals, antipedals, etc., derived from N-periodics has added to our list of invariants (we are now at some 80 entries) [17]. A particular prolific object has been the focus-inversive polygon, shown in see Figure 3. Its vertices are the inversions of N-periodic vertices with respect to a unit-circle centered on a focus. Though the inversive family is inscribed in Pascal's Limaçon, a surprising experimental observation is that like N-periodics, the inversive perimeter and sum of cosines are also invariant for all N [17, k803,k804].

Referring to Figures 7 and 14, here we also explore properties of self-intersected N-periodics which exist for all $N > 3$. Namely, if an invariant works for a simple orbit, will it also work in the self-intersected case?

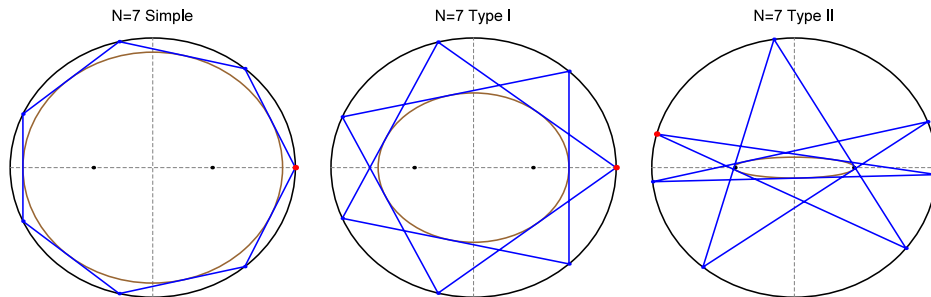


FIGURE 4. Three types of 7-periodics in an $a/b = 1.1$ elliptic billiard, namely: (i) non-intersecting, (ii) self-intersected type I (turning number 2), (iii) self-intersected type II (turning number 3). [Video 1](#), [Video 2](#)

Main contributions:

- Section 2: Focus-inversive 3-periodics are a constant-perimeter family inscribed in a rigidly moving ellipse, i.e., a moving elliptic billiard.
- Section 3: The vertices of self-intersected 4-periodics and their outer polygon are concyclic with the foci on two distinct variable-radius circles.
- Section 4: for $N=3,4,6,8$, we derive expressions for selected invariants listed in [17] including a few self-intersecting cases.
- In Appendix B.4 (resp. B.6) we show that the caustic semi-axes for $N=5$ ($N=7$) periodics, simple or self-intersected, are roots of degree-6 (resp. degree-12) polynomials. There are two valid cases for $N = 5$ and 3 for $N = 7$; see Figure 4.

Since many phenomena are best understood in motion, a link is provided in the caption of most figures to an animation. Table 2 in Section 5 compiles all videos mentioned and a few extra ones.

In Appendix A we review some classical quantities for the Billiard. In Appendix B we provide explicit expressions for vertices and caustics for $N = 3, 4, 5, 6, 7, 8$ in both simple and self-intersected configurations. In Appendix C we list all symbols used.

2. $N=3$ INVERSIVE FAMILY IS NEW BILLIARD FAMILY

Throughout this article we assume the elliptic billiard is the ellipse:

$$(1) \quad f(x, y) = \left(\frac{x}{a}\right)^2 + \left(\frac{y}{b}\right)^2 = 1, \quad a > b > 0.$$

A generic $N > 3$ focus-inversive polygon is illustrated in Figure 3. This is a polygon whose vertices are inversions of the N -periodic vertices wrt a circle of radius ρ centered on f_1 .

It is well known the inversion of an ellipse wrt to a focus is Pascal's Limaçon [9]. Therefore, for any N :

Remark 1. *The focus-inversive family is inscribed in Pascal's Limaçon.*

Figure 5 illustrates the $N = 3$ focus-inversive triangle. Recall two well-known triangle centers: the Gergonne point X_7 is the perspector of the incircle and the

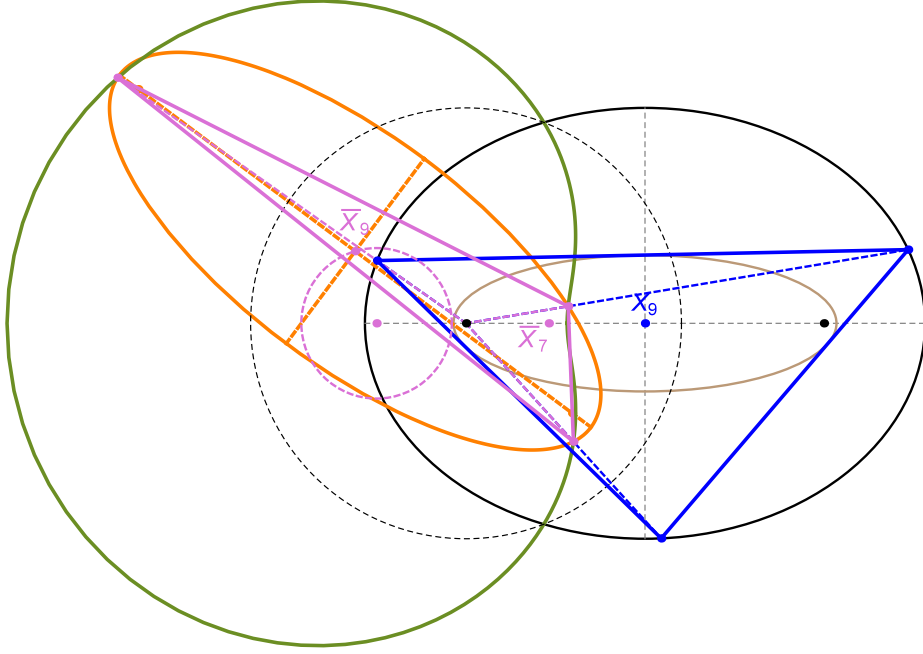


FIGURE 5. The vertices of 3-periodics (blue), when inverted with respect to a unit circle (dashed black) centered on a focus, produce a family of constant perimeter triangles (pink). Their X_9 -centered circumellipses (orange) rigidly translate and rotate (invariant semi-axes) with their center (\bar{X}_9) moving along a circle. The Gergonne point \bar{X}_7 of the inversive family is stationary. [Video](#)

Mittenpunkt X_9 is the point of concurrence of lines drawn from the excenters through the medians [13].

Proposition 1. *Over the 3-periodic family, the Gergonne point X_7 of its focus-inversive triangles is stationary on the billiard's major axis.*

Proposition 2. *Over the 3-periodic family, the Mittenpunkt X_9 of its focus-inversive triangles moves along a circle whose center lies on the billiard's major axis.*

Note: we omit explicit expressions for the two previous results since they would occupy several pages.

Proposition 3. *The X_9 -centered circumellipse \mathcal{C}^\dagger of the $N = 3$ inversive family has invariant semi-axes a^\dagger and b^\dagger given by:*

$$\begin{aligned}
a^\dagger &= \rho k_1 \sqrt{a c k_2 + \delta (2 a^2 - b^2 - \delta)} \\
b^\dagger &= \rho k_1 \sqrt{-a c k_2 + \delta (2 a^2 - b^2 - \delta)} \\
k_1 &= \frac{c\sqrt{2}}{k_3} \sqrt{(8 a^4 + 4 a^2 b^2 + 2 b^4) \delta + 8 a^6 + 3 a^2 b^4 + 2 b^6} \\
k_2 &= \sqrt{(-4 a^2 + 2 b^2) \delta + 5 a^4 - 5 a^2 b^2 + 2 b^4} \\
k_3 &= 2 a b^2 ((2 a^2 - b^2) \delta + 2 a^4 - 2 a^2 b^2 - b^4)
\end{aligned}$$

Note: \mathcal{C}^\dagger is the rigidly-moving circumbilliard [16] of the inversive polygon.

Proposition 4. *The perimeter L^\dagger of the $N=3$ focus-inversive family is invariant and given by:*

$$L^\dagger = \rho \frac{\sqrt{(8 a^4 + 4 a^2 b^2 + 2 b^4) \delta + 8 a^6 + 3 a^2 b^4 + 2 b^6}}{a^2 b^2}$$

In turn, the above entail:

Theorem 1. *With respect to a reference system centered on \bar{X}_9 and oriented along the semi-axes of \mathcal{C}^\dagger , the inversive $N = 3$ family is a 3-periodic billiard family of \mathcal{C}^\dagger .*

Experimentally we have observed:

Conjecture 1. *The perimeter of the focus-inversive polygon is invariant for any N .*

3. VERTICES $N=4$ SELF-INTERSECTED ARE CONCYCLIC WITH FOCI

The family of non-self-intersected (simple) billiard 4-periodics is comprised of parallelograms [7]. In this section consider self-intersected 4-periodics whose caustic is a confocal hyperbola; see Figure 7. We start deriving simple facts about them and then proceed to certain elegant properties.

Proposition 5. *The perimeter L of the self-intersected 4-periodic is given by:*

$$(2) \quad L = \frac{4a^2}{c}, \quad \text{with } c^2 = a^2 - b^2.$$

Proof. Since perimeter is constant, use as the $N = 4$ candidate the centrally-symmetric one, Figure 6 (right). Its upper-right vertex $P_1 = (x_1, y_1)$ is such that it reflects a vertical ray toward $-P_1$, and this yields:

$$P_1 = (x_1, y_1) = \left[\frac{a\sqrt{a^2 - 2b^2}}{bc}, \frac{b}{c} \right]$$

Since $P_2 = -P_1$ its perimeter is $L = 2(|2P_1| + 2y_1)$ and this can be simplified to (2), invariant over the family. \square

with $a/b \geq \sqrt{2}$. At $a/b = \sqrt{2}$ the family is a straight line from top to bottom vertex of the EB, Figure 6 (left).

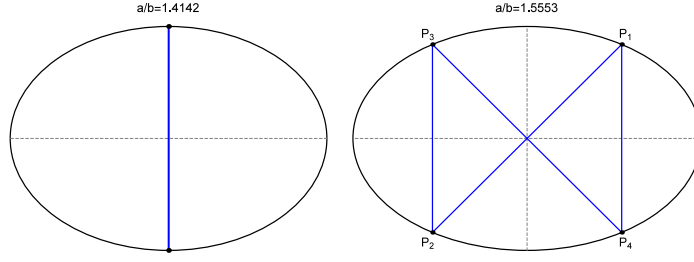


FIGURE 6. Self-intersected 4-periodic (blue) in its central position (symmetric about the minor and major axes of the EB). **Left:** $a/b = \sqrt{2}$, the orbit is a generate vertical segments. **Right:** $a/b \simeq 1.55377$, the orbit's perimeter is identical to the EB's. [Video](#)

Observation 1. At $a/b = \sqrt{1 + \sqrt{2}} \simeq 1.55377$ the two self-intersecting segments of the bowtie do so at right-angles.

Observation 2. At $a/b \simeq 1.55529$ the perimeter of the bowtie equal that of the EB.

Referring to Figure 7:

Proposition 6. The $N = 4$ self-intersected family has zero signed orbit area and zero sum of signed cosines, i.e., both are invariant. The same two facts are true for its outer polygon.

Proof. This stems from the fact all self-intersected 4-periodics are symmetric with respect to the EB's minor axis. \square

Referring to Figure 7, as in Appendix B.2, let vertex P_1 of the self-intersected 4-periodic be parametrized as $P_1(u) = [au, b\sqrt{1-u^2}]$, with $|u| \leq \frac{a}{c^2} \sqrt{a^2 - 2b^2}$. Then:

Theorem 2. The four vertices of the self-intersected 4-periodic (resp. outer polygon) are concyclic with the two foci of the elliptic billiard, on a circle \mathcal{C} of variable radius R (resp. R') whose center C (resp. C') lies on the y axis. These are given by:

$$\begin{aligned} C &= \left[0, \frac{c^2 u^2 - a^2 + 2b^2}{2b\sqrt{1-u^2}} \right] \\ R &= \frac{a^2 - c^2 u^2}{2b\sqrt{1-u^2}} \\ C' &= \left[0, -\frac{2bc^2\sqrt{1-u^2}}{a^2 + (u^2 - 2)c^2} \right] \\ R' &= \frac{c(c^2 u^2 - a^2)}{a^2 - 2c^2 + c^2 u^2} \end{aligned}$$

Corollary 1. The half harmonic mean of R^2 and R'^2 is invariant and equal to $c^2 = a^2 - b^2$, i.e., $1/R^2 + 1/R'^2 = 1/c^2$.

Note: the above Pythagorean relation implies that the polygon whose vertices are a focus, and the inversion of C, C', O (center of billiard) with respect to a unit circle centered on said focus, is a rectangle of sides $1/R$ and $1/R'$ and diagonal $1/c$.

Let \mathcal{P}^\dagger (resp. \mathcal{Q}^\dagger) denote the inversive polygon of 4-periodics (resp. its outer polygon) wrt a unit circle \mathcal{C}^\dagger centered on one focus. From properties of inversion:

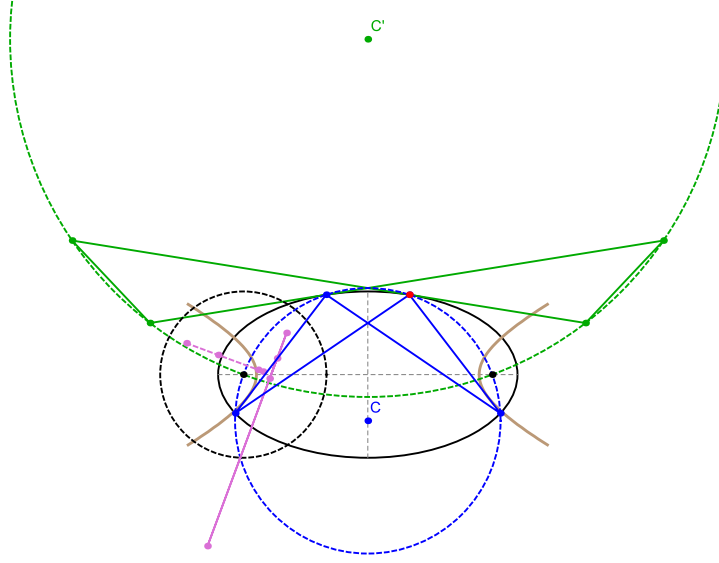


FIGURE 7. The vertices of the self-intersected 4-periodic (blue) are concyclic with the billiard foci on a circle (dashed blue) centered on C . The inversive polygon (pink segment) with respect to a unit circle C^\dagger (dashed black) centered on the left focus degenerates to a segment along the radical axis of the two circles. The vertices of the outer polygon (green) are also concyclic with the foci on a distinct circle (dashed green) centered on C' . Therefore the outer's inversive polygon (dotted pink) is also a segment along the radical axis of this circle with C^\dagger . Note the two radical axes are dynamically perpendicular. [Video 1](#), [Video 2](#)

Corollary 2. \mathcal{P}^\dagger (resp. \mathcal{Q}^\dagger) has four collinear vertices, i.e., it degenerates to a segment along the radical axis of C^\dagger and C (resp. C').

Proposition 7. The two said radical axes are perpendicular.

Proof. It is enough to check that the vectors $C - [-c, 0]$ and $C' - [-c, 0]$ are orthogonal. Observe that when $u^2 = (a^2 - 2b^2)/c = (2c^2 - a^2)/c$ the outer polygon is contained in the horizontal axis. \square

4. DERIVING INVARIANTS FOR $N=3,4,5,6,8$

In this section, we derive expressions for selected invariants introduced in [17], specifically for “low- N ” cases, e.g., $N=3,4,5,6,8$. In that publication, each invariant is identified by a 3-digit code, e.g., k_{101} , k_{102} , etc. Table 1 lists the invariants considered herein. The quantities involved are defined next.

Let θ_i denote the i th N -periodic angle. Let A the signed area of an N -periodic. Referring to Figure 2, singly-primed quantities (e.g., θ'_i , A' , etc.), etc., always refer to the *outer polygon*: its sides are tangent to the EB at the P_i . Likewise, doubly-primed quantities (θ''_i , A'' , etc.) refer to the *inner polygon*: its vertices lie at the touchpoints of N -periodic sides with the caustic. More details on said quantities appear in Appendix A.

Recall $k_{101} = JL - N$, as introduced in [18, 4].

code	invariant	valid N	derived	proofs
k_{101}	$\sum \cos \theta_i$	all	n/a	[2, 4]
k_{102}	$\prod \cos \theta'_i$	all	3,4,5,5 _i ,6,6 _i ,6 _{ii}	[2, 4]
k_{103}	A'/A	odd	3,5,5 _i	[2, 6]
k_{104}	$\sum \cos(2\theta'_i)$	all	3,4,5,5 _i ,6,6 _i ,8	[1]
k_{105}	$\prod \sin(\theta_i/2)$	odd	3,5,5 _i	[1]
k_{106}	$A'A$	even	4,6,6 _i ,6 _{ii}	[6]
k_{110}	AA''	even	4,6,6 _i ,6 _{ii}	?
$^\dagger k_{119}$	$\sum \kappa_i^{2/3}$	all	3,4,6	[2, 19]
$k_{802,a}$	$\sum 1/d_{1,i}$	all	3,4,6	[2]
k_{803}	L_1^\dagger	all	3,4,6	?
$^\dagger k_{804}$	$\sum \cos \theta_{1,i}^\dagger$	$\neq 4$	3	?
$k_{805,a}$	AA_1^\dagger	$\equiv 0 \pmod{4}$	4,8	?
k_{806}	A/A_1^\dagger	$\equiv 2 \pmod{4}$	6	?
k_{807}	$A_1^\dagger A_2^\dagger$	odd	3	?

TABLE 1. List of selected invariants taken from [17] as well as the low-N cases (column “derived”) for expressions are derived herein. † co-discovered with P. Roitman. A closed-form expression for k_{119} was derived by H. Stachel; see (5).

Referring to Figure 3, the f_1 -*inversive polygon* has vertices at inversions of the P_i with respect to a unit circle centered on f_1 . Quantities such as L_1^\dagger , A_1^\dagger , etc., refer to perimeter, area, etc. of said polygon.

A word about our proof method. We omit most proofs as they have been produced by a consistent process, namely: (i) using the expressions in Appendix B, find the vertices an axis-symmetric N-periodic, i.e., whose first vertex $P_1 = (a, 0)$; (ii) obtain a symbolic expression for the invariant of interest, (iii) simplify it (both human intervention and CAS), and finally (iv) verify its validity numerically over several N-periodic configurations and elliptic billiard aspect ratios a/b .

4.1. Invariants for N=3. Let $\delta = \sqrt{a^4 - a^2b^2 + b^4}$. For $N = 3$ explicit expressions for J and L have been derived [11]:

$$(3) \quad \begin{aligned} J &= \frac{\sqrt{2\delta - a^2 - b^2}}{c^2} \\ L &= 2(\delta + a^2 + b^2)J \end{aligned}$$

When $a = b$, $J = \sqrt{3}/2$ and when $a/b \rightarrow \infty$, $J \rightarrow 0$.

Proposition 8. For $N = 3$, $k_{102} = (JL)/4 - 1$.

Proof. We’ve shown $\sum_{i=1}^3 \cos \theta_i = JL - 3$ is invariant for the $N = 3$ family [11]. For any triangle $\sum_{i=1}^3 \cos \theta_i = 1 + r/R$ [21], so it follows that $r/R = JL - 4$ is also invariant. Let r_h, R_h be the Orthic Triangle’s Inradius and Circumradius. The relation $r_h/R_h = 4 \prod_{i=1}^3 |\cos \theta_i|$ is well-known [21, Orthic Triangle]. Since a

triangle is the Orthic of its Excentral Triangle, we can write $r/R = 4 \prod_{i=1}^3 \cos \theta'_i$, where θ'_i are the Excentral angles which are always acute [21] (absolute value can be dropped), yielding the claim. \square

Proposition 9. For $N = 3$, $k_{103} = k_{109} = 2/(k_{101} - 1) = 2/(JL - 4)$.

Proof. Given a triangle A' (resp. A'') refers to the area of the Excentral (resp. Extouch) triangles. The ratios A'/A and A/A'' are equal. Actually, $A'/A = A/A'' = (s_1 s_2 s_3)/(r^2 L)$, where s_i are the sides, L the perimeter, and r the Inradius [21, Excentral, Extouch]. Also known is that $A'/A = 2R/r$ [12]. Since $r/R = \sum_{i=1}^3 \cos \theta_i - 1 = k_{101} - 1$ [21, Inradius], the result follows. \square

Proposition 10. For $N = 3$, $k_{104} = -k_{101}$ and is given by:

$$k_{104} = \frac{(a^2 + b^2)(a^2 + b^2 - 2\delta)}{c^4} = 3 - JL$$

Proposition 11. For $N = 3$, $k_{105} = (JL)/4 - 1 = k_{102}$.

Proof. Let r, R be a triangle's Inradius and Circumradius. The identity $r/R = 4 \prod_{i=1}^3 \sin(\theta_i/2)$ holds for any triangle [21, Inradius], which with Proposition 8 This completes the proof. \square

Proposition 12. For $N = 3$, k_{119} is given by:

$$(k_{119})^3 = \frac{2J^3 L}{(JL - 4)^2}, \quad k_{119} = \frac{a^2 + b^2 + \delta}{(ab)^{\frac{4}{3}}}$$

Proof. Use the expressions for L, J in (3). \square

Proposition 13. For $N = 3$, $k_{802,a}$ is given by:

$$k_{802,a} = \frac{a^2 + b^2 + \delta}{ab^2} = \frac{J\sqrt{2}\sqrt{JL + \sqrt{9 - 2JL} - 3}}{JL - 4}$$

Remark 2. For $N = 3$, k_{803} was given in Proposition 4.

Proposition 14. For $N = 3$, k_{804} is given by:

$$k_{804} = \frac{\delta(a^2 + c^2 - \delta)}{a^2 c^2}$$

Proposition 15. For $N = 3$, k_{807} is given by:

$$k_{807} = \frac{\rho^8}{8a^8 b^2} \left[(a^4 + 2a^2 b^2 + 4b^4) \delta + a^6 + (3/2) a^4 b^2 + 4b^6 \right]$$

r is the radius of the inversion circle, included above for unit consistency. By default $r = 1$.

4.2. Invariants for N=4.

Proposition 16. *For $N = 4$, $k_{102} = 0$.*

Proof. Non-self-intersecting 4-periodics are parallelograms [7] whose outer polygon is a rectangle inscribed in Monge's Orthoptic Circle [18]. This finishes the proof. \square

Proposition 17. *For $N = 4$, $k_{104} = -4$.*

Proof. As in Proposition 16, outer polygon is a rectangle. \square

Proposition 18. *For $N = 4$, $k_{106} = 8a^2b^2$.*

Proposition 19. *For $N = 4$, k_{110} is given by $\frac{2a^4b^4}{(a^2+b^2)^2}$*

Let $\kappa_a = (ab)^{-2/3}$ is the affine curvature of the ellipse and $r_m = \sqrt{a^2 + b^2}$ the radius of Monge's orthoptic circle [21].

Proposition 20. *For $N = 4$, $k_{119} = \frac{2(a^2+b^2)}{(ab)^{\frac{4}{3}}} = 2(\kappa_a r_m)^2$*

Proposition 21. *For $N = 4$, $k_{802,a} = \frac{2(a^2+b^2)}{ab^2}$*

Proposition 22. *For $N = 4$, $k_{803} = \frac{4\sqrt{a^2+b^2}}{b^2}$*

Observation 3. *Experimentally, k_{804} is invariant for all non-intersecting N -periodics, except for $N = 4$.*

Proposition 23. *For $N = 4$, $k_{805,a} = 4$*

Note: see Section 3 for a treatment of N=4 self-intersected geometry.

4.3. Invariants for N=5. As seen in Appendix B, the vertices of 5-periodics can only be obtained via an implicitly-defined caustic. I.e., we first numerically obtain the caustic semi-axes and then compute a axis-symmetric polygon tangent to it. Note that both simple and self-intersected 5-periodics possess an elliptic confocal caustic; see Figure 8.

Proposition 24. *For $N = 5$ simple (resp. self-intersected), k_{102} is given by the largest negative (resp. positive) real root of the following sextic:*

$$\begin{aligned} k_{102} : & 1024c^{20}x^6 + 2048(a^4 + a^3b - ab^3 + b^4)(a^4 - a^3b + ab^3 + b^4)c^{12}x^5 \\ & + 256(4a^{12} - a^{10}b^2 + 32a^8b^4 - 22a^6b^6 + 32a^4b^8 - a^2b^{10} + 4b^{12})c^8x^4 \\ & - 64a^2b^2(4a^{12} - 27a^{10}b^2 + 38a^8b^4 - 126a^6b^6 + 38a^4b^8 - 27a^2b^{10} + 4b^{12})c^4x^3 \\ & - 16a^6b^6(7a^8 - 96a^6b^2 + 114a^4b^4 - 96a^2b^6 + 7b^8)x^2 \\ & - 8a^8b^8(7a^4 + 30a^2b^2 + 7b^4)x - a^{10}b^{10} = 0 \end{aligned}$$

Proposition 25. *For $N = 5$ simple (resp. self-intersected), k_{103} is given by the smallest (resp. largest) real root greater than 1 of the following sextic:*

$$\begin{aligned} k_{103} : & a^6b^6x^6 - 2b^2a^2(4a^8 - a^6b^2 - a^2b^6 + 4b^8)x^5 \\ & - b^2a^2(4a^8 + 19a^6b^2 - 62a^4b^4 + 19a^2b^6 + 4b^8)x^4 \\ & + 12b^2a^2(a^4 + b^4)c^4x^3 + (4a^8 + 19a^6b^2 + 66a^4b^4 + 19a^2b^6 + 4b^8)c^4x^2 \\ & + (2a^8 + 12a^6b^2 + 36a^4b^4 + 12a^2b^6 + 2b^8)c^4x - c^{12} \end{aligned}$$

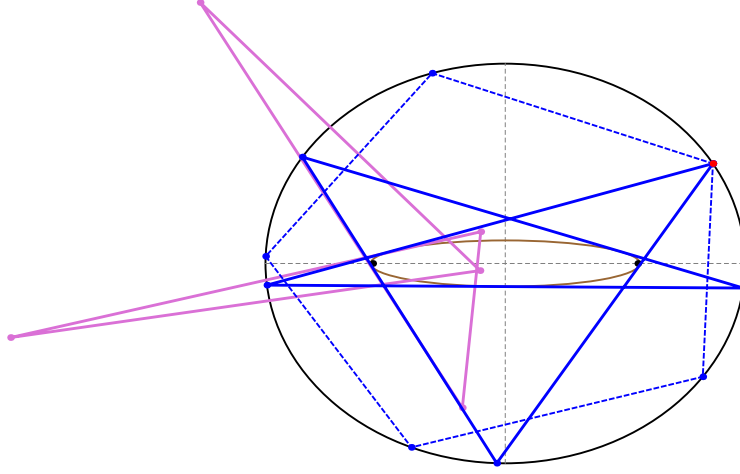


FIGURE 8. A simple (blue) and self-intersected (dashed blue) 5-periodic, as well as the former's focus-inversive polygon (pink). [Video](#)

Proposition 26. For $N = 5$ simple (resp. self-intersected), k_{104} is given by the only negative (resp. smallest largest) real root of the following sextic:

$$\begin{aligned} & c^{12}x^6 - 2(a^4 + 10a^2b^2 + b^4)c^8x^5 - (37a^4 - 6a^2b^2 + 37b^4)c^8x^4 \\ & + 4(5a^8 + 92a^6b^2 + 62a^4b^4 + 92a^2b^6 + 5b^8)c^4x^3 \\ & + (423a^{12} - 354a^{10}b^2 + 2713a^8b^4 - 4796a^6b^6 + 2713a^4b^8 - 354a^2b^{10} + 423b^{12})x^2 \\ & + (270a^{12} + 740a^{10}b^2 - 3630a^8b^4 + 7160a^6b^6 - 3630a^4b^8 + 740a^2b^{10} + 270b^{12})x \\ & - 675a^{12} - 850a^{10}b^2 + 1075a^8b^4 - 3900a^6b^6 + 1075a^4b^8 - 850a^2b^{10} - 675b^{12} = 0 \end{aligned}$$

Proposition 27. For $N = 5$ simple (resp. self-intersected), k_{105} is given by the largest positive real root (resp. the symmetric value of the largest negative root) of the following sextic:

$$\begin{aligned} & 2^{10}c^{20}x^6 + 2^{10}(2a^{12} + a^{10}b^2 + 26a^8b^4 + 70a^6b^6 + 26a^4b^8 + a^2b^{10} + 2b^{12})c^8x^5 \\ & + 2^8(4a^{12} + 30a^{10}b^2 + 71a^8b^4 + 350a^6b^6 + 71a^4b^8 + 30a^2b^{10} + 4b^{12})c^8x^4 \\ & + 2^6a^2b^2(4a^{12} + 9a^{10}b^2 - 318a^8b^4 - 126a^6b^6 - 318a^4b^8 + 9a^2b^{10} + 4b^{12})c^4x^3 \\ & - 2^6a^2b^2(8a^{16} - 53a^{14}b^2 + 253a^{12}b^4 - 1041a^{10}b^6 + 1650a^8b^8 \\ & - 1041a^6b^{10} + 253a^4b^{12} - 53a^2b^{14} + 8b^{16})x^2 \\ & - 2^4a^2b^2(16a^{16} - 12a^{14}b^2 + 5a^{12}b^4 + a^{10}b^6 + 2a^8b^8 + a^6b^{10} + 5a^4b^{12} - 12a^2b^{14} + 16b^{16})x \\ & - a^{10}b^{10} = 0 \end{aligned}$$

4.4. **Invariants for $N=6$.** Referring to Figure 2 (right):

Proposition 28. For $N = 6$, $k_{102} = a^2b^2/(4(a+b)^4) = (JL - 4)^2/64$.

Proposition 29. For $N = 6$, $k_{104} = k_{101} = JL - 6$.

Proposition 30. For $N = 6$, k_{106} is given by:

N=6 self-intersected type I

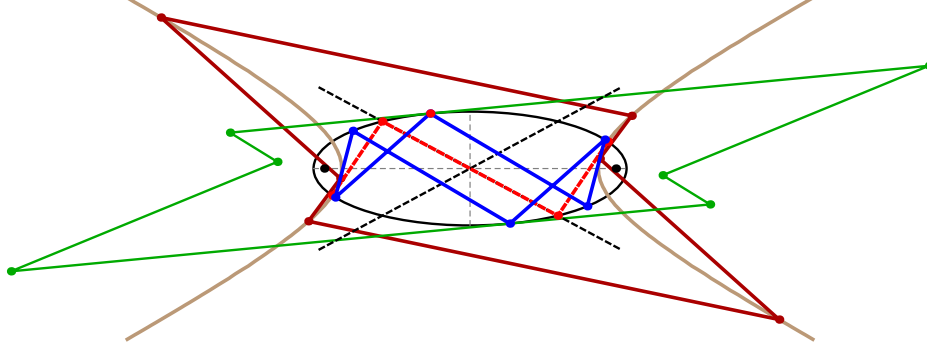


FIGURE 9. Type I self-intersected 6-periodic (blue) and its doubled-up configuration (dashed red), both tangent to a hyperbolic confocal caustic (brown). Its asymptotes (dashed black) pass through the center of the EB. Also shown are the outer (green) and inner (dark red) polygons. [Video](#)

$$k_{106} = \frac{4b^2(2a+b)a^2(a+2b)}{(a+b)^2} = -\frac{(JL-12)(JL-4)^2}{16J^4}$$

Proposition 31. For $N = 6$, k_{110} is given by:

$$k_{110} = \frac{4a^3b^3(2a+b)^2(a+2b)^2}{(a+b)^6} = -\frac{(JL-12)^2(JL-4)^3}{256J^4}$$

Proposition 32. For $N = 6$, $k_{119}^3 = \frac{2^5 J^5 L^3}{(JL-4)^4}$

Proposition 33. For $N = 6$, $k_{802,a} = \frac{2(a^2+ab+b^2)}{ab^2} = \frac{4J^2L(1+\sqrt{JL-3})}{(JL-4)^2}$

Proposition 34. For $N = 6$, $k_{803} = 2\rho^2(2a^2 + 2ab - b^2)/(ab^2)$.

Proposition 35. For $N = 6$, $k_{806} = 4\rho^{-4}a^3b^4/((2a-b)(a+b)^2)$.

Referring to Figure 9:

4.5. N=6 self-intersecting. Take a regular hexagon. There are 60 orderings with which to connect its vertices (modulo rotations and chirality); see [21, Pascal Lines].

It turns out only two $N = 6$ topologies can produce closed trajectories, both with two self-intersections. These will be referred to as type I and type II, and are depicted in Figures 9, and 10, respectively.

Proposition 36. For $N = 6$ type I, $k_{102} = a^2b^2/(4(a-b)^4) = (JL-4)^2/64$

Proposition 37. For $N = 6$ type II,

$$k_{102} = a^2(a-c)^2/(4c^4) = (JL-8)^2(JL-4)^2/1024$$

Proposition 38. For $N = 6$ type I, $k_{104} = -\frac{2(a^2-4ab+b^2)}{(a-b)^2} = JL-6 = k_{101}$.

N=6 self-intersected type II

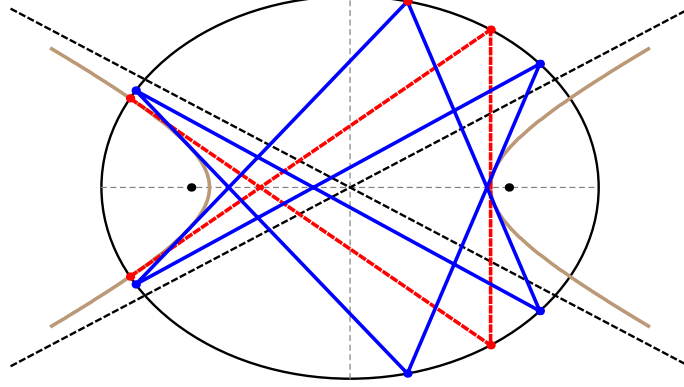


FIGURE 10. Self-intersected 6-periodic (type II) shown both at one of its doubled-up configurations (dashed red) and in general position (blue). Segments are tangent to a hyperbolic confocal caustic (brown) whose asymptotes (dashed black) pass through the center of the EB. Also shown is the outer polygon (green) which in this case is always simple. [Video](#)

Note that $k_{104} = k_{101} = JL - 6$ for both $N = 6$ simple and type I. However:

Proposition 39. *For $N = 6$ type II,*

$$k_{104} = \frac{2(a^2 - ac + c^2)(a^2 - ac - c^2)}{c^4} = \frac{(J^2L^2 - 12JL + 16)(J^2L^2 - 12JL + 48)}{128}$$

Proposition 40. *For $N = 6$ type I, $k_{106} = 4a^2b^2(a - 2b)(2a - b)/(a - b)^2 = -(JL - 12)(JL - 4)^2/(16J^4)$*

Proposition 41. *For $N = 6$ type I,*

$$k_{110} = \frac{-4a^3b^3(a - 2b)^2(2a - b)^2}{(a - b)^6} = \frac{(JL - 12)^2(JL - 4)^3}{2^8 J^4}$$

Proposition 42. *For $N = 6$ type II, both A and A' vanish, and therefore $k_{106} = 0$ and $k_{110} = 0$.*

Observation 4. *Experimentally, k_{804} is invariant for $N = 6$ simple, and type I. However, it is variable for $N = 6$ type II.*

4.6. **Invariants for N=8.** Referring to Figure 11:

Proposition 43. *For $N = 8$, k_{102} is given by $(1/2^{12})(JL - 4)^2(JL - 12)^2$.*

Referring to Figure 11:

Proposition 44. *For $N = 8$, $k_{104} = 0$.*

Proof. Using the CAS, we checked that k_{104} vanishes for an 8-periodic in the “horizontal” position, i.e., $P_1 = (a, 0)$. Since k_{104} is invariant [2], this completes the proof. \square

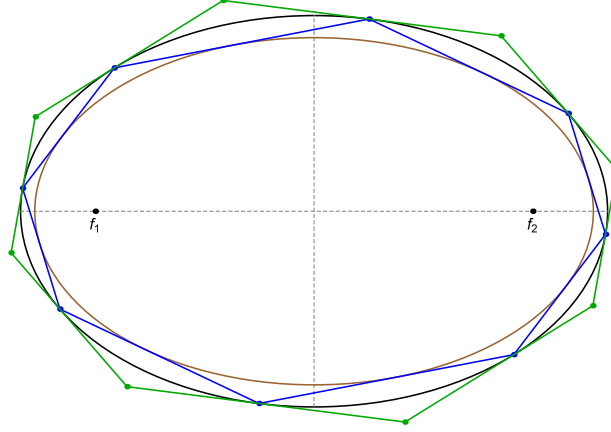


FIGURE 11. The outer polygon (green) to an 8-periodic has null sum of double cosines. [Video](#)

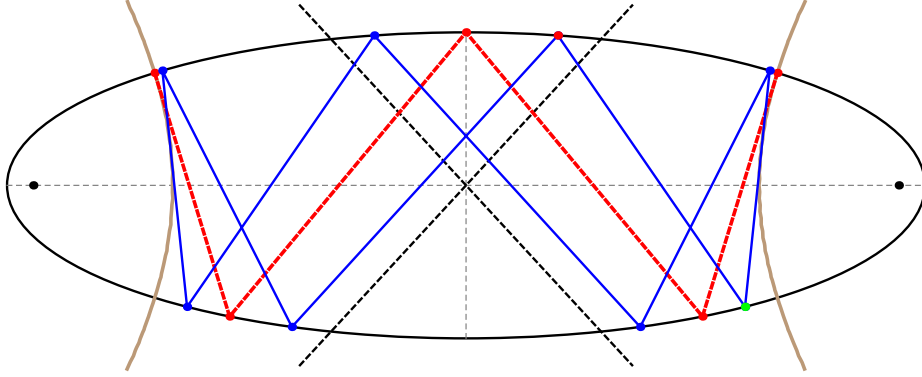


FIGURE 12. Self-intersecting 8-periodic of type I (blue) and its doubled-up configuration (dashed red) in $a/b = 3$ ellipse. Trajectory segments are tangent to a confocal hyperbolic caustic (brown). [Video](#)

4.7. $N=8$ Self-Intersected. There are 3 types of self-intersected 8-periodics [5], here called type I, II, and III. These correspond to trajectories with turning numbers of 0, 2, and 3, respectively. These are depicted in Figures 12, 13, and 14.

Observation 5. *The signed area of $N = 8$ type I is zero.*

Referring to Figure 14, the following is related to the Poncelet Grid [14] and the Hexagramma Mysticum [3]:

Observation 6. *The outer polygon to $N=8$ type III is inscribed in an ellipse.*

5. VIDEOS

Animations illustrating some of the above phenomena are listed on Table 2.

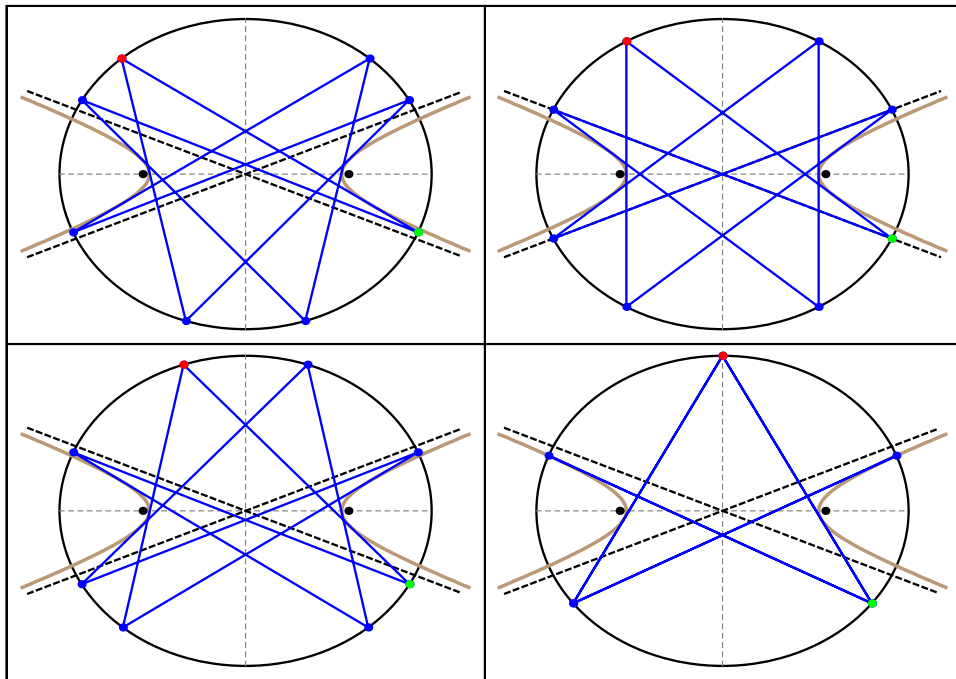


FIGURE 13. Four positions of a type II self-intersecting 8-periodic (blue) in an $a/b = 1.2$ elliptic billiard, at four different locations of a starting vertex (red). In general position, these have turning number 2. Also shown is confocal hyperbolic caustic (brown). [Video](#)

ACKNOWLEDGMENTS

We would like to thank Jair Koiller, Arseniy Akopyan, Richard Schwartz, Sergei Tabachnikov, Pedro Roitman, and Hellmuth Stachel for useful insights.

The first author is fellow of CNPq and coordinator of Project PRONEX/ CNPq/ FAPEG 2017 10 26 7000 508.

APPENDIX A. BILLIARD RECAP

Joachimsthal's Integral expresses that every trajectory segment is tangent to a confocal caustic [20]. Equivalently, a positive quantity J remains invariant at every bounce point $P_i = (x_i, y_i)$:

$$J = \frac{1}{2} \nabla f_i \cdot \hat{v} = \frac{1}{2} |\nabla f_i| \cos \alpha$$

where \hat{v} is the unit incoming (or outgoing) velocity vector, and:

$$\nabla f_i = 2 \left(\frac{x_i}{a^2}, \frac{y_i}{b^2} \right).$$

Hellmuth Stachel contributed [19] an elegant expression for Joahmisthal's constant J in terms of EB semiaxes a, b and the major semiaxes a'' of the caustic:

$$J = \frac{\sqrt{a^2 - a''^2}}{ab}$$

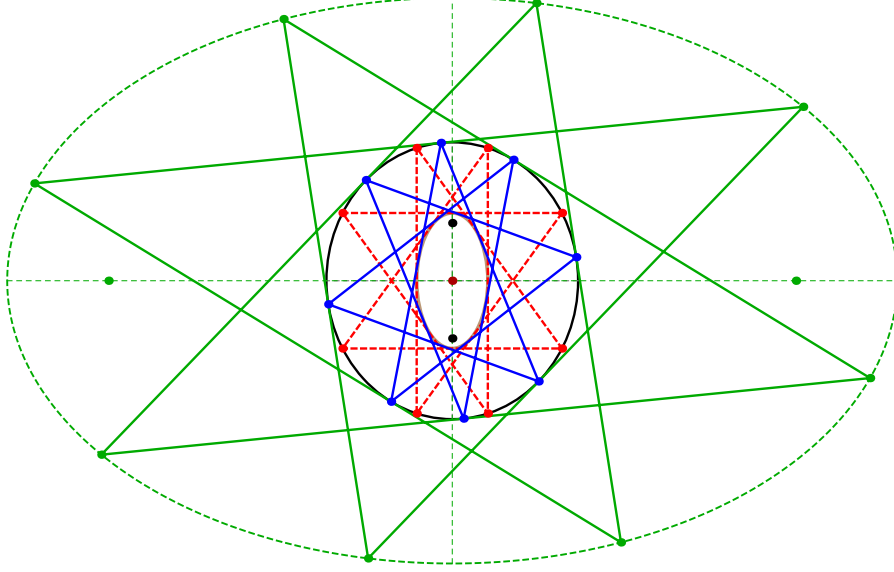


FIGURE 14. Self-intersecting 8-periodic of type III (blue) and its doubled-up configuration (dashed red) in an $a/b = 1.1$ billiard ellipse (shown rotated by 90° to save space). The turning number is 3. The confocal caustic is an ellipse (brown). Also shown is the outer polygon (green) whose vertices are inscribed in an axis-aligned, concentric ellipse (dashed green), a result related to [3]. [Video](#)

Let κ_i denote the curvature of the EB at P_i given by [21, Ellipse]:

$$(4) \quad \kappa = \frac{1}{a^2 b^2} \left(\frac{x^2}{a^4} + \frac{y^2}{b^4} \right)^{-3/2}$$

The signed area of a polygon is given by the following sum of cross-products [15]:

$$A = \frac{1}{2} \sum_{i=1}^N (P_{i+1} - P_i) \times (P_i - P_{i+1})$$

Let $d_{j,i}$ be the distance $|P_i - f_j|$. The inversion $P_{j,i}^\dagger$ of vertex P_i with respect to a circle of radius ρ centered on f_j is given by:

$$P_{j,i}^\dagger = f_j + \left(\frac{\rho}{d_{j,i}} \right)^2 (P_i - f_j)$$

The following closed-form expression for k_{119} for all N was contributed by H. Stachel [19]:

$$(5) \quad \sum_{i=1}^N \kappa_i^{2/3} = L/[2J(ab)^{4/3}]$$

id	Title	youtu.be/<...>
01	N=3-6 orbits and caustics	Y3q35D0bfZU
02	N=5 with inner and outer polygons	PRkhrUNTxd8
03	N=6 zero-area antipedal @ $a/b = 2$	HMhZW_kWLGw
04	N=8 outer poly's null sum of double cosines	GEmV_U4eRIE
05	N=4 self-int. and its outer polygon	C8W2e6ftf0w
06	N=4 self-int. vertices concyclic w/ foci	207Ta31P19I
07	N=4 self-int. vertices and outer concyclic w/ foci	4g-JBshX10U
08	N=5 self-int. (pentagram)	ECe4DptduJY
09	N=6 self-int. type I	f0D85MnrmdQ
10	N=6 self-int. type II	gQ-FbSq7wWY
11	N=7 self-int. type I and II	yzBG8rgPUP4
12	N=8 self-int. type I	5Lt9atsZhRs
13	N=8 self-int. type II	3xpGnDxyi0
14	N=8 self-int. type III	JwD_w5ecPYs
15	N=3 inversives rigidly-moving circumbilliard	L0JK5izTctI
16	N=3 inversive: invariant area product	OL2uMk2xyKk
17	N=5 inversives: invariant area product	bTkbdEPNUOY
18	N=5 self-int. inversive: invariant perimenter	LuLtbwxfSbc
19	N=5 and outer inversives: invariant area ratio	eG4UCgMkK18
20	N=7 self-int. type I inversives: invariant area product	BRQ3909ogNE

TABLE 2. Videos illustrating some concepts in the article. The last column provides a YouTube code.

APPENDIX B. VERTICES & CAUSTICS N=3,4,5,6,8

B.1. N=3 Vertices & Caustic. Let $P_i = (x_i, y_i)/q_i$, $i = 1, 2, 3$, denote the 3-periodic vertices, given by [10]:

$$\begin{aligned}
q_1 &= 1 \\
x_2 &= -b^4 ((a^2 + b^2) k_1 - a^2) x_1^3 - 2a^4 b^2 k_2 x_1^2 y_1 \\
&\quad + a^4 ((a^2 - 3b^2) k_1 + b^2) x_1 y_1^2 - 2a^6 k_2 y_1^3 \\
y_2 &= 2b^6 k_2 x_1^3 + b^4 ((b^2 - 3a^2) k_1 + a^2) x_1^2 y_1 \\
&\quad + 2a^2 b^4 k_2 x_1 y_1^2 - a^4 ((a^2 + b^2) k_1 - b^2) y_1^3 \\
q_2 &= b^4 (a^2 - c^2 k_1) x_1^2 + a^4 (b^2 + c^2 k_1) y_1^2 - 2a^2 b^2 c^2 k_2 x_1 y_1 \\
x_3 &= b^4 (a^2 - (b^2 + a^2)) k_1 x_1^3 + 2a^4 b^2 k_2 x_1^2 y_1 \\
&\quad + a^4 (k_1 (a^2 - 3b^2) + b^2) x_1 y_1^2 + 2a^6 k_2 y_1^3 \\
y_3 &= -2b^6 k_2 x_1^3 + b^4 (a^2 + (b^2 - 3a^2) k_1) x_1^2 y_1 \\
&\quad - 2a^2 b^4 k_2 x_1 y_1^2 + a^4 (b^2 - (b^2 + a^2) k_1) y_1^3, \\
q_3 &= b^4 (a^2 - c^2 k_1) x_1^2 + a^4 (b^2 + c^2 k_1) y_1^2 + 2a^2 b^2 c^2 k_2 x_1 y_1.
\end{aligned}$$

where:

$$\begin{aligned}
k_1 &= \frac{d_1^2 \delta_1^2}{d_2} = \cos^2 \alpha, \\
k_2 &= \frac{\delta_1 d_1^2}{d_2} \sqrt{d_2 - d_1^4 \delta_1^2} = \sin \alpha \cos \alpha \\
c^2 &= a^2 - b^2, \quad d_1 = (a b/c)^2, \quad d_2 = b^4 x_1^2 + a^4 y_1^2 \\
\delta &= \sqrt{a^4 + b^4 - a^2 b^2}, \quad \delta_1 = \sqrt{2\delta - a^2 - b^2}
\end{aligned}$$

where α , though not used here, is the angle of segment $P_1 P_2$ (and $P_1 P_3$) with respect to the normal at P_1 .

The caustic is the ellipse:

$$\frac{x^2}{a''^2} + \frac{y^2}{b''^2} - 1 = 0, \quad a'' = \frac{a(\delta - b^2)}{a^2 - b^2}, \quad b'' = \frac{b(a^2 - \delta)}{a^2 - b^2}$$

B.2. N=4 Vertices & Caustic.

B.3. Simple. The vertices of the 4-periodic orbit are given by:

$$\begin{aligned}
P_1 &= (x_1, y_1), \quad P_2 = \left(-\frac{a^4 y_1}{\sqrt{b^6 x_1^2 + a^6 y_1^2}}, \frac{b^4 x_1}{\sqrt{b^6 x_1^2 + a^6 y_1^2}} \right) \\
P_3 &= -P_1, \quad P_4 = -P_2
\end{aligned}$$

The caustic is the ellipse:

$$\frac{x^2}{a''^2} + \frac{y^2}{b''^2} - 1 = 0, \quad a'' = \frac{a^2}{\sqrt{a^2 + b^2}}, \quad b'' = \frac{b^2}{\sqrt{a^2 + b^2}}$$

The area and its bounds are given by:

$$A = \frac{2(b^4 x_1^2 + a^4 y_1^2)}{\sqrt{b^6 x_1^2 + a^6 y_1^2}}, \quad \frac{4a^2 b^2}{a^2 + b^2} \leq A \leq 2ab$$

The minimum (resp. maximum) area is achieved when the orbit is a rectangle with $P_1 = (x_1, b^2 x_1/a^2)$ (resp. rhombus with $P_1 = (a, 0)$).

The perimeter is given by:

$$L = 4\sqrt{a^2 + b^2}$$

The exit angle α required to close the trajectory from a departing position (x_1, y_1) on the billiard boundary is given by:

$$\cos \alpha = \frac{a^2 b}{\sqrt{a^2 + b^2} \sqrt{a^4 - c^2 x_1^2}}$$

B.3.1. *Self-intersected.* When $a/b > \sqrt{2}$, the vertices of the 4-periodic self-intersecting orbit are given by:

$$\begin{aligned} P_1 &= [au, b\sqrt{1-u^2}], \quad P_3 = [-au, b\sqrt{1-u^2}] \\ P_2 &= \left[-\frac{a\sqrt{a^2(a^2-2b^2)-c^4u^2}}{c^2\sqrt{1-u^2}}, -\frac{b^3}{c^2\sqrt{1-u^2}} \right] \\ P_4 &= \left[\frac{a\sqrt{a^2(a^2-2b^2)-c^4u^2}}{c^2\sqrt{1-u^2}}, -\frac{b^3}{c^2\sqrt{1-u^2}} \right] \end{aligned}$$

where $|u| \leq \frac{a}{c^2} \sqrt{a^2 - 2b^2}$.

The confocal hyperbolic caustic is given by:

$$\frac{x^2}{a''^2} - \frac{y^2}{b''^2} = 1, \quad a'' = \frac{a\sqrt{a^2-2b^2}}{c}, \quad b'' = \frac{b^2}{c}$$

The four intersections of the caustic and the EB are given by:

$$\left[\pm \frac{a^2\sqrt{a^2-2b^2}}{c^2}, \pm \frac{b^3}{c^2} \right]$$

The exit angle α required to close the trajectory from a departing position (x_1, y_1) on the billiard boundary is given by:

$$\cos \alpha = \frac{a^2b}{c\sqrt{a^4 - c^2x_1^2}}$$

The perimeter of the orbit is $L = 4a^2/c$.

B.4. N=5 Vertices & Caustic. Let $a > b$ be the semi-axes of the elliptic billiard. Consider a 5-periodic with vertices $P_i, i = 1, \dots, 5$ where P_1 is at $(a, 0)$, i.e., the orbit is “horizontal”.

Proposition 45. *The major semiaxis length a'' of the caustic for $N = 5$ non-intersecting (resp. intersecting, i.e., pentagram) is given by the root of the largest (resp. smallest) real root $x \in (0, a)$ of the following bi-sextic polynomial:*

$$\begin{aligned} P_5(x) &= c^{12}x^{12} - 2c^4a^2(3a^8 - 9a^6b^2 + 31a^4b^4 + a^2b^6 + 6b^8)x^{10} \\ &\quad + c^4a^4(15a^8 - 30a^6b^2 + 191a^4b^4 + 16a^2b^6 + 16b^8)x^8 \\ &\quad - 4c^4a^{10}(5a^4 - 5a^2b^2 + 66b^4)x^6 \\ &\quad + a^{12}(15a^8 - 30a^6b^2 + 191a^4b^4 - 368a^2b^6 + 208b^8)x^4 \\ &\quad - 2a^{14}(3a^8 - 3a^6b^2 + 22a^4b^4 - 48a^2b^6 + 32b^8)x^2 + a^{24} \end{aligned}$$

Proof. The polynomial P_5 is exactly the Cayley condition for the existence of 5-periodic orbits, see [8]. For $c = 0$ the roots are $a'_2 = (\sqrt{5} - 1)a/4$ and $a''_2 = (\sqrt{5} + 1)a/4$ and corresponds to the regular case. For $b = 0$ the roots are coincident in given by $x = a$. By analytic continuation, for $c \in (0, a)$, the two roots are in the interval $(0, a)$. \square

For $N = 5$ non-intersecting, the abscissae of vertices $P_2 = (x_2, y_2)$, $P_3 = (x_3, y_3)$ are given by the smallest positive solution (resp. unique negative) of the following equations:

$$\begin{aligned} x_2 : & c^6 x_2^6 - 2a(2a^2 - b^2)c^4 x_2^5 + a^2(5a^2 + 4b^2)c^4 x_2^4 - 8a^5 b^2 c^2 x_2^3 \\ & - a^8(5a^2 - 9b^2)x_2^2 + 2a^9(2a^2 - b^2)x_2 - a^{12} = 0 \\ x_3 : & c^6 x_3^6 - 2ab^2 c^2(3a^2 + b^2)x_3^5 - a^2 c^2(3a^4 - 3a^2 b^2 + 4b^4)x_3^4 + 12a^5 b^2 c^2 x_3^3 \\ & + a^6(3a^4 - 3a^2 b^2 + 4b^4)x_3^2 - 2a^7 b^2(3a^2 - 4b^2)x_3 - a^{12} = 0 \end{aligned}$$

The Joachimstall invariant J of the simple orbit is given by the small positive root of

$$\begin{aligned} & 4096c^{12}J^{12} + 2048(3a^2 + b^2)(a^2 + 3b^2)(a^2 + b^2)c^4 J^{10} \\ & - 256(29a^4 + 54a^2 b^2 + 29b^4)c^4 J^8 + 2304(a^2 + b^2)c^4 J^6 \\ & - 16(3a^2 - 4ab - 3b^2)(3a^2 + 4ab - 3b^2)J^4 - 40(a^2 + b^2)J^2 + 5 = 0 \end{aligned}$$

The perimeter of the simple orbit is given by

$$\begin{aligned} L &= \frac{p}{q} \\ p &= (1024(a^2 + b^2)c^4 b^2 J^7 - 256c^4 b^2 J^5 - 64(a^2 + b^2)b^2 J^3 + 16Jb^2)\sqrt{1 - 4a^2 J^2} \\ & - 1024c^2(5a^4 + 2a^2 b^2 + b^4)b^2 J^7 + 256c^2(3a^2 + b^2)b^2 J^5 + 64c^2 b^2 J^3 + 16Jb^2 \\ q &= 256c^8 J^8 - 256c^2(a^2 + b^2)^2 J^6 + 32c^2(3a^2 + 5b^2)J^4 - 16c^2 J^2 + 1 \end{aligned}$$

B.5. N=6 Vertices & Caustic.

B.5.1. *Simple.* Vertices $P_i, i = 2, \dots, 6$ with $P_1 = (a, 0)$ are given by:

$$\begin{aligned} P_4 &= [-a, 0] \\ P_2 &= [k_x, k_y], \quad P_5 = -P_2 \\ P_3 &= [-k_x, k_y], \quad P_6 = -P_3 \\ k_x &= \frac{a^2}{a+b}, \quad k_y = \frac{b\sqrt{b(2a+b)}}{a+b} \end{aligned}$$

The confocal, elliptic caustic is given by:

$$\frac{x^2}{a''^2} + \frac{y^2}{b''^2} = 1, \quad a'' = \frac{a\sqrt{a(a+2b)}}{a+b}, \quad b'' = \frac{b\sqrt{b(2a+b)}}{a+b}$$

The perimeter is given by:

$$L = \frac{4(a^2 + ab + b^2)}{a+b}$$

B.5.2. *Self-Intersected (type I)*. This orbit only exists for $a > 2b$. Vertices $P_i, i = 2, \dots, 6$ with $P_1 = (0, b)$ are given by:

$$\begin{aligned} P_4 &= [0, -b] \\ P_2 &= [k_x, k_y], \quad P_5 = -P_2 \\ P_3 &= [k_x, -k_y], \quad P_6 = -P_3 \\ k_x &= \frac{a\sqrt{a(a-2b)}}{b-a}, \quad k_y = \frac{b^2}{b-a} \end{aligned}$$

The confocal, hyperbolic caustic is given by:

$$\frac{x^2}{a''^2} - \frac{y^2}{b''^2} = 1, \quad a'' = \frac{a^{3/2}\sqrt{a-2b}}{a-b}, \quad b'' = \frac{b^{3/2}\sqrt{2a-b}}{a-b}$$

The 4 intersections (x_{int}, y_{int}) of the caustic with the EB are given by:

$$[x_{int}, y_{int}] = \left[\pm \sqrt{\frac{a^5(a-2b)}{(a-b)^3(a+b)}}, \pm \sqrt{\frac{b^5(b-2a)}{(b-a)^3(a+b)}} \right]$$

The perimeter is given by:

$$L = \frac{4(a^2 - ab + b^2)}{a-b}$$

B.5.3. *Self-Intersected (type II)*. This orbit only exists for $a > \frac{2b\sqrt{3}}{3}$. Vertices $P_i, i = 2, \dots, 6$ with $P_1 = [0, b]$ are given by: are given by:

$$\begin{aligned} P_4 &= [0, -b] \\ P_2 &= [k_x, k_y], \quad P_3 = -P_2 \\ P_5 &= [k_x, -k_y], \quad P_6 = -P_5 \\ k_x &= -\frac{a^{\frac{3}{2}}\sqrt{2c-a}}{c}, \quad k_y = \frac{(c-a)b}{c} \end{aligned}$$

The confocal hyperbolic caustic is given by:

$$\frac{x^2}{a''^2} - \frac{y^2}{b''^2} = 1, \quad a''^2 = \frac{a^3(3ac-2b^2)}{c(3a^2+b^2)}, \quad b''^2 = \frac{b^2(2a^2(a-c)-b^2c)}{c(3a^2+b^2)}$$

The 4 intersections (x_{int}, y_{int}) of the caustic with the EB are given by:

$$[x_{int}, y_{int}] = \left[\pm \frac{a}{c} \sqrt{\frac{a(3ac-2b^2)}{c(3a^2+b^2)}}, \pm \frac{b^2}{c} \sqrt{\frac{3a^2(a-c)+c^3}{c(3a^2+b^2)}} \right]$$

The perimeter is given by:

$$L = 4(a+c)\sqrt{2a/c-1}$$

B.6. N=7 Caustic. Referring to Figure 4, there are three types of 7-periodics: (i) non-intersecting, (ii) self-intersecting type I, i.e., with turning number 2, (iii) self-intersecting type II.

Proposition 46. *The caustic semiaxis for non-intersecting 7-periodics (resp. self-intersecting type I, and type II self-intersecting) are given by the smallest (resp. second and third smallest) root of the following degree-12 polynomial:*

$$\begin{aligned} & c^{12}x_1^{12} - 4(a^2 + b^2)c^6a(3a^2 + b^2)b^2x_1^{11} \\ & - 2c^6a^2(3a^6 - 6a^4b^2 + 13a^2b^4 - 2b^6)x_1^{10} + (60a^4 + 60b^2a^2 + 8b^4)c^6a^3x_1^9 \\ & + a^6c^2(15a^8 - 45a^6b^2 + 125a^4b^4 - 143a^2b^6 + 112b^8)x_1^8 - 8a^7b^2c^2(15a^6 - 20a^4b^2 - 7a^2b^4 + 8b^6)x_1^7 \\ & - 4a^8c^2(5a^8 - 10a^6b^2 + 35a^4b^4 - 30a^2b^6 + 36b^8)x_1^6 + 8a^9b^2c^2(15a^6 - 25a^4b^2 - 2a^2b^4 + 4b^6)x_1^5 \\ & + a^{10}c^2(15a^8 - 15a^6b^2 + 80a^4b^4 - 32a^2b^6 + 64b^8)x_1^4 - 4a^{15}b^2(15a^4 - 45b^2a^2 + 32b^4)x_1^3 \\ & - 2a^{16}(3a^6 - 3a^4b^2 + 10a^2b^4 - 8b^6)x_1^2 + 4a^{17}b^2(3a^2 - 4b^2)(a^2 - 2b^2)x_1 + a^{24} = 0 \end{aligned}$$

It can shown the first two smallest (resp. third smallest) roots of the above polynomial are negative (resp. positive), and all have absolute values within $(0, a)$.

For $a = b$ the polynomial equation above is given by $a^3 + 4a^2x_1 - 4ax_1^2 - 8x_1^3 = 0$ with roots $-0.9009688680a$, $-0.2225209340a$, $0.6234898025a$.

B.7. N=8 Vertices & Caustic.

B.7.1. Simple. Vertices $P_i, i = 1, \dots, 8$ with $P_1 = [a, 0]$ are given by:

$$\begin{aligned} P_1 &= [a, 0], \quad P_5 = -[a, 0], \quad P_3 = [0, b], \quad P_7 = [0, -b] \\ P_{2,4,6,8} &= [\pm ax, \pm b\sqrt{1-x^2}], \text{ where } x \text{ is a positive root of:} \\ c^4x^4 - 2a^2c^2x^3 + 2a^2b^2x^2 + 2a^2c^2x - a^4 &= 0 \end{aligned}$$

B.7.2. Self-Intersected (type I and type II). These have hyperbolic confocal caustics; see Figures 12, 13. Let $P_1 = (x_1, y_1)$ be at the intersection of the hyperbolic caustic with the billiard for each case. For type I (resp. type II) x_1 is given by the smallest (resp. largest) positive root $x_1 \in (0, a)$ of the following degree-8 polynomial:

$$\begin{aligned} x_1 : & c^{16}x_1^8 - 4a^4c^8(a^6 - 4a^4b^2 + a^2b^4 - 2b^6)x_1^6 + 2a^8c^6(3a^6 - 15a^4b^2 - 4b^6)x_1^4 \\ & - 4a^{16}c^4(a^2 - 6b^2)x_1^2 + a^{20}(a^4 - 8a^2b^2 + 8b^4) = 0 \end{aligned}$$

B.7.3. Self-Intersected (type III). Let $P_1 = (x_1, y_1)$ and $P_2 = (x_1, -y_1)$ be two consecutive vertices in the doubled-up type III 8-periodic (dashed red in Figure 14) connected by a vertical line (the figure is rotated, therefore this line will appear horizontal). x_1^2 is given by the smallest positive root of the following quartic polynomial on ω :

$$\begin{aligned} x_1 : & (a^4 + 6a^2b^2 + b^4)c^4x_1^8 - 4a^4(a^2 + 5b^2)c^4x_1^6 + 2a^6(3a^6 + 6a^4b^2 - 21a^2b^4 + 16b^6)x_1^4 \\ & - 4a^8(a^6 + a^4b^2 - 4a^2b^4 + 4b^6)x_1^2 + a^{16} = 0 \\ x_1 : & \alpha^{16} + (\alpha^2 - 1)^2(\alpha^4 + 6\alpha^2 + 1)\omega^4 - 4(\alpha^2 - 1)^2(\alpha^2 + 5)\alpha^4\omega^3 + \\ & 2(3(\alpha^4 + 2\alpha^2 - 7)\alpha^2 + 16)\alpha^6\omega^2 - 4(\alpha^6 + \alpha^4 - 4\alpha^2 + 4)\alpha^8\omega = 0 \end{aligned}$$

where $\alpha = a/b$.

APPENDIX C. TABLE OF SYMBOLS

symbol	meaning
O, N	center of billiard and vertex count
L, J	inv. perimeter and Joachimsthal's constant
a, b	billiard major, minor semi-axes
a'', b''	caustic major, minor semi-axes
f_1, f_2	foci
P_i, P'_i, P''_i	N -periodic, outer, inner polygon vertices
$d_{j,i}$	distance $ P_i - f_j $
κ_i	ellipse curvature at P_i
θ_i, θ'_i	N -periodic, outer polygon angles
A, A', A''	N -periodic, outer, inner areas
ρ	radius of the inversion circle
$P_{j,i}^\dagger$	vertices of the inversive polygon wrt f_j
$L_{j,i}^\dagger, A_j^\dagger$	perimeter, area of inversive polygon wrt f_j
$\theta_{j,i}^\dagger$	i th angle of inversive polygon wrt f_j

TABLE 3. Symbols used in the invariants. Note $i \in [1, N]$ and $j = 1, 2$.

REFERENCES

- [1] Akopyan, A. (2020). Corollary of Theorem 6 in Akopyan et al., “Billiards in Ellipses Revisited” (2020). Private Communication.
- [2] Akopyan, A., Schwartz, R., Tabachnikov, S. (2020). Billiards in ellipses revisited. *Eur. J. Math.* doi.org/10.1007/s40879-020-00426-9.
- [3] Baralić, D., Spasojević, I. (2015). Illumination of Pascal’s Hexagrammum and Octagrammum Mysticum. *Discrete & Computational Geometry*, 53(2).
- [4] Bialy, M., Tabachnikov, S. (2020). Dan Reznik’s identities and more. *Eur. J. Math.* doi.org/10.1007/s40879-020-00428-7.
- [5] Birkhoff, G. (1927). On the periodic motions of dynamical systems. *Acta Mathematica*, 50(1): 359–379. doi.org/10.1007/BF02421325.
- [6] Chavez-Caliz, A. (2020). More about areas and centers of Poncelet polygons. *Arnold Math J.* doi.org/10.1007/s40598-020-00154-8.
- [7] Connes, A., Zagier, D. (2007). A property of parallelograms inscribed in ellipses. *The American Mathematical Monthly*, 114(10): 909–914. bit.ly/3okmvjM.
- [8] Dragović, V., Radnović, M. (2011). *Poncelet Porisms and Beyond: Integrable Billiards, Hyperelliptic Jacobians and Pencils of Quadrics*. Frontiers in Mathematics. Basel: Springer.
- [9] Ferréol, R. (2020). Pascal’s limaçon. Mathcurve Portal. <https://mathcurve.com/courbes2d.gb/limaçon/limaçon.shtml>.
- [10] Garcia, R. (2019). Elliptic billiards and ellipses associated to the 3-periodic orbits. *American Mathematical Monthly*, 126(06): 491–504.
- [11] Garcia, R., Reznik, D., Koiller, J. (2020). New properties of triangular orbits in elliptic billiards. *Amer. Math. Monthly*, to appear.
- [12] Johnson, R. A. (1929). *Modern Geometry: An Elementary Treatise on the Geometry of the Triangle and the Circle*. Boston, MA: Houghton Mifflin.
- [13] Kimberling, C. (2019). Encyclopedia of triangle centers. faculty.evansville.edu/ck6/encyclopedia/ETC.html.

- [14] Levi, M., Tabachnikov, S. (2007). The Poncelet grid and billiards in ellipses. *The American Mathematical Monthly*, 114(10): 895–908. doi.org/10.1080/00029890.2007.11920482.
- [15] Preparata, F., Shamos, M. (1988). *Computational Geometry - An Introduction*. Springer-Verlag, 2nd ed.
- [16] Reznik, D., Garcia, R. (2021). Circuminvariants of 3-periodics in the elliptic billiard. *Intl. J. Geometry*, 10(1): 31–57.
- [17] Reznik, D., Garcia, R., Koiller, J. Fifty new invariants of n-periodics in the elliptic billiard. To appear.
- [18] Reznik, D., Garcia, R., Koiller, J. (2020). Can the elliptic billiard still surprise us? *Math Intelligencer*, 42: 6–17. rdcu.be/b2cg1.
- [19] Stachel, H. (2020). Private Communication.
- [20] Tabachnikov, S. (2005). *Geometry and Billiards*, vol. 30 of *Student Mathematical Library*. Providence, RI: American Mathematical Society. bit.ly/2RV04CK.
- [21] Weisstein, E. (2019). Mathworld. mathworld.wolfram.com.